

## Spectral phonon scattering effects on the thermal conductivity of nano-grained barium titanate

Brian F. Donovan, Brian M. Foley, Jon F. Ihlefeld, Jon-Paul Maria, and Patrick E. Hopkins

Citation: [Applied Physics Letters](#) **105**, 082907 (2014); doi: 10.1063/1.4893920

View online: <http://dx.doi.org/10.1063/1.4893920>

View Table of Contents: <http://scitation.aip.org/content/aip/journal/apl/105/8?ver=pdfcov>

Published by the [AIP Publishing](#)

---

### Articles you may be interested in

[Thermal conductivity of nano-grained SrTiO<sub>3</sub> thin films](#)

Appl. Phys. Lett. **101**, 231908 (2012); 10.1063/1.4769448

[Effective medium formulation for phonon transport analysis of nanograined polycrystals](#)

J. Appl. Phys. **111**, 014307 (2012); 10.1063/1.3675273

[Effect of grain sizes and shapes on phonon thermal conductivity of bulk thermoelectric materials](#)

J. Appl. Phys. **110**, 024312 (2011); 10.1063/1.3611421

[Thermal transport and grain boundary conductance in ultrananocrystalline diamond thin films](#)

J. Appl. Phys. **99**, 114301 (2006); 10.1063/1.2199974

[Impact of grain sizes on phonon thermal conductivity of bulk thermoelectric materials](#)

Appl. Phys. Lett. **87**, 242101 (2005); 10.1063/1.2137463

---



**computing**  
IN SCIENCE & ENGINEERING

AIP's JOURNAL OF COMPUTATIONAL TOOLS AND METHODS.  
**AVAILABLE AT MOST LIBRARIES.**

## Spectral phonon scattering effects on the thermal conductivity of nano-grained barium titanate

Brian F. Donovan,<sup>1</sup> Brian M. Foley,<sup>2</sup> Jon F. Ihlefeld,<sup>3,a)</sup> Jon-Paul Maria,<sup>4</sup> and Patrick E. Hopkins<sup>2,b)</sup>

<sup>1</sup>*Department of Material Science and Engineering, University of Virginia, Charlottesville, Virginia 22904, USA*

<sup>2</sup>*Department of Mechanical and Aerospace Engineering, University of Virginia, Charlottesville, Virginia 22904, USA*

<sup>3</sup>*Electronic, Optical, and Nanomaterials Department, Sandia National Laboratories, Albuquerque, New Mexico 87185, USA*

<sup>4</sup>*Department of Material Science and Engineering, North Carolina State University, Raleigh, North Carolina 27695, USA*

(Received 30 April 2014; accepted 9 August 2014; published online 27 August 2014)

We study the effect of grain size on thermal conductivity of thin film barium titanate over temperatures ranging from 200 to 500 K. We show that the thermal conductivity of Barium Titanate ( $\text{BaTiO}_3$ ) decreases with decreasing grain size as a result of increased phonon scattering from grain boundaries. We analyze our results with a model for thermal conductivity that incorporates a spectrum of mean free paths in  $\text{BaTiO}_3$ . In contrast to the common gray mean free path assumption, our findings suggest that the thermal conductivity of complex oxide perovskites is driven by a spectrum of phonons with varying mean free paths. © 2014 AIP Publishing LLC.

[<http://dx.doi.org/10.1063/1.4893920>]

Barium titanate ( $\text{BaTiO}_3$ ) is a widely used material in the electronics and ceramics industry due to its favorable and well known dielectric and ferroelectric properties.<sup>1–4</sup> For example,  $\text{BaTiO}_3$  is the primary constituent in multilayer ceramic capacitors,<sup>5</sup> a multi-billion dollar industry that necessitates size scaling of their components into the nanometer range for continued growth.<sup>6</sup> While the dielectric and structural properties of  $\text{BaTiO}_3$  have been widely studied, less is known about the thermal properties. Relatively large discrepancies in the reputed values of the thermal conductivity of  $\text{BaTiO}_3$  currently exist in literature; particularly, sub-micron-grained samples show wide variation in the reported thermal conductivity. Having a robust understanding of the effects of nano-scale features on thermal properties is of paramount importance as devices and device packaging continue to scale.

In a previous work,<sup>7</sup> we have studied the role of phonon scattering mechanisms on the room temperature thermal conductivity in nano-grained  $\text{SrTiO}_3$ . We determined that in this simple perovskite system with a cubic crystal structure, grain sizes as large as 100 nm can reduce the thermal conductivity of thin film  $\text{SrTiO}_3$ , alluding to the relative lengths scales of heat carrying mean free paths in this complex oxide. This result suggested that a gray approximation to phonon transport may not be valid in ferroelectric oxides.<sup>8–10</sup> This begs the question whether a spectrum of mean free paths will contribute to the thermal conductivity in ferroelectric materials with more complex crystal structures and complicated atomic arrangements.  $\text{BaTiO}_3$  represents an ideal material system to study complex phonon scattering mechanisms and their role on thermal conductivity in a complex oxide;  $\text{BaTiO}_3$ , a non-centrosymmetric system, exhibits dynamic

changes in crystal symmetry between 200 and 500 K, the temperature range of interest in this study as well as the aforementioned device and industrial applications. The various phases of  $\text{BaTiO}_3$  exhibit a variety of Brillouin zone shapes and sizes, resulting in changes to the phonon dispersion as temperature varies across phase transitions. The phonon transport processes in  $\text{BaTiO}_3$  with varying grain sizes across a range of temperatures therefore will give insight into the fundamental thermal scattering mechanisms and length scales dictating thermal conductivity in  $\text{BaTiO}_3$  and other ferroelectric perovskites.

To understand phonon scattering mechanisms and their effects on thermal conductivity in  $\text{BaTiO}_3$ , we study the influence of grain size on thermal conductivity in thin films over temperatures ranging from 200 to 500 K. We synthesize a series of nanograined (ng)  $\text{BaTiO}_3$  thin films via chemical solution deposition<sup>11</sup> and measure their thermal conductivities with time domain thermoreflectance (TDTR).<sup>12–14</sup> We show a consistent trend in the thermal conductivity of the  $\text{BaTiO}_3$  films as a function of grain size, similar to what we have previously observed in nanograined  $\text{SrTiO}_3$  films; we note that this consistency in the effects of nano-structuring on the thermal conductivity of  $\text{BaTiO}_3$  does not appear among previous works.<sup>15,16</sup> Our data agree well with predictions for the grain boundary scattering effects on the thermal conductivity of  $\text{BaTiO}_3$  using a simplified semi-classical model. The temperature trends suggest that phonon-boundary scattering events, both at grains and the film/substrate boundary, are the dominant source of thermal resistance. This is in line with our model, which assumes a spectrally dependent phonon mean free path in the  $\text{BaTiO}_3$  system. The influence of 36–63 nm diameter grains on the thermal conductivity of  $\text{BaTiO}_3$  indicates that phonons with this characteristic length scale can contribute to the thermal conductivity of single crystal  $\text{BaTiO}_3$ ,

<sup>a)</sup>Electronic mail: jihlefe@sandia.gov

<sup>b)</sup>Electronic mail: phopkins@virginia.edu

which is contrary to the typical kinetic theory calculation of the  $\sim 2$  nm mean free path assuming a gray medium. Therefore, our work demonstrates the spectral nature of the thermal mean free paths of phonons in BaTiO<sub>3</sub> with typical length scales well beyond that predicted by a gray approximation using kinetic theory.<sup>17</sup>

In contrast to the variety of conflicting values in current works in literature, our work elucidates the effects of grain size on thermal conductivity of thin films of BaTiO<sub>3</sub> using a robust measurement technique, not susceptible to radiative loss, and a consistent sample set with uniform film thickness and well characterized materials. The current literature values regarding the effects of nano-structuring on BaTiO<sub>3</sub> range from studies with 150 nm grains exhibiting near-bulk thermal conductivities of  $5.1 \text{ W m}^{-1} \text{ K}^{-1}$  (Ref. 16) to studies with grain sizes of 100 nm exhibiting thermal conductivities of  $10.22 \text{ W m}^{-1} \text{ K}^{-1}$ , which is over twice that reported for the bulk thermal conductivity of BaTiO<sub>3</sub>.<sup>18</sup> See supplementary material for further discussion of these current discrepancies in the literature.<sup>19</sup> Utilizing the sensitivity of TDTR and well understood processing with full characterization of our materials, we are able to clearly show the effects of grain boundaries on the thermal conductivity of BaTiO<sub>3</sub> and illustrate the typical length scales of the thermal phonon mean free paths in the system. Taken with our previous work on SrTiO<sub>3</sub>,<sup>7</sup> our body of work suggests the spectral nature of phonons in complex oxide perovskites in general.

BaTiO<sub>3</sub> thin films were prepared via chemical solution deposition utilizing a varying final anneal temperature to modify the final grain size.<sup>20</sup> A chelate chemistry comprising barium acetate, titanium isopropoxide, acetylacetonate, propionic acid, and methanol was used and is described in more detail in prior work.<sup>21</sup> Cation precursors were assayed prior to batching to ensure a stoichiometric composition. A single film was spin cast onto a polished polycrystalline alumina substrate (CoorsTek Superstrate), which was chosen to minimize potential texturing effects that may occur due to local epitaxy with a sapphire substrate. Films nine layers in total thickness (ca.  $\sim 175$  nm as-fired thickness) were prepared with an 800 °C anneal after every layer to assure that all carbonaceous species are removed and that a dense film is prepared.<sup>11,22</sup> The substrate was then diced and each section is annealed at temperatures between 850 and 1000 °C in 50 °C increments for 1 h in air to modify the grain size.

A 175 nm thick epitaxial BaTiO<sub>3</sub> film was grown on a (001)-oriented SrTiO<sub>3</sub> single crystalline substrate via 30° off-axis RF magnetron sputtering from a 75 mm diameter sintered BaTiO<sub>3</sub> target. The SrTiO<sub>3</sub> surface was prepared with a TiO<sub>2</sub> termination prior to growth.<sup>23</sup> The film was grown with a substrate temperature of 700 °C in a 20 mTorr, 5:1 ratio argon:oxygen atmosphere with a growth rate of 2.7 nm/min. The film was allowed to cool in the growth atmosphere to minimize the formation of oxygen point defects.

Film phase assemblage and orientation were assessed with X-ray diffraction using a Philips X'Pert MPD instrument with copper K $\alpha$  radiation. Figure 1 shows representative X-ray diffraction patterns for each film. In each case, a phase pure film is identified. The solution deposited films possess no preferred orientation and therefore can be considered randomly oriented and polycrystalline. The epitaxial

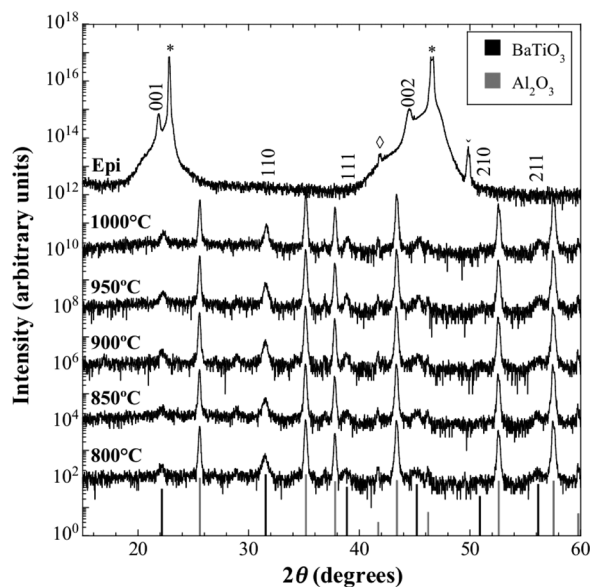


FIG. 1. X-ray diffraction patterns for BaTiO<sub>3</sub> films processed between 800 and 1000 °C on polycrystalline alumina substrates and an epitaxial film prepared on a 001-oriented SrTiO<sub>3</sub> substrate. The bar markers indicate peak positions for cubic BaTiO<sub>3</sub> (Ref. 25) and corundum structured Al<sub>2</sub>O<sub>3</sub> (Ref. 26). \* denotes SrTiO<sub>3</sub> reflections,  $\diamond$  denotes a reflection of copper K $\beta$  radiation, and  $\dagger$  is an unknown peak that we have previously observed for these SrTiO<sub>3</sub> substrates and this diffractometer and is not believed to be a secondary phase in the film.

film possesses peaks consistent with *c*-axis oriented BaTiO<sub>3</sub>. No evidence of other *a*-axis or reflections from other planes could be observed. Rocking curves measured for the substrate and film 002 peaks possessed full width at half maximum values of 0.092° and 1.142°, respectively. See supplementary material for further detail on the material analysis conducted in this study. The increased width of the film peak can be attributed to strain fields around misfit dislocations near the film/substrate interface.<sup>24</sup>

Film microstructure was assessed with scanning electron microscopy (Zeiss Supra 55VP in in-lens imaging mode and FEI Varios) and atomic force microscopy (Park Scientific Autoprobe CP). Figure 2 shows scanning electron micrographs of the polycrystalline films after annealing at the different temperatures. A clear increase in grain size with increasing annealing temperature is observed. Cross-sectional images reveal relatively dense microstructures (>97% based upon image analysis, ImageJ, National Institutes of Health) for each condition and smooth interfaces with the substrate. Average grain sizes were assessed from the atomic force microscope images using the linear intercept method.<sup>27</sup> Error bars on the grain size measurements represent 95% confidence intervals.

We measured the thermal conductivity of the nano-grained films with time domain thermoreflectance.<sup>12–14</sup> See supplementary material for details of the TDTR experiment, specific parameters of our measurement, and corresponding thermal analysis and assumptions.<sup>19</sup> The thermal conductivities of the nano-grained thin films were greatly reduced compared with bulk values. Furthermore, the average size of the grains in each sample significantly affected its thermal conductivity. A clear reduction in the thermal conductivity of the ng-BaTiO<sub>3</sub> compared with the epitaxial film is

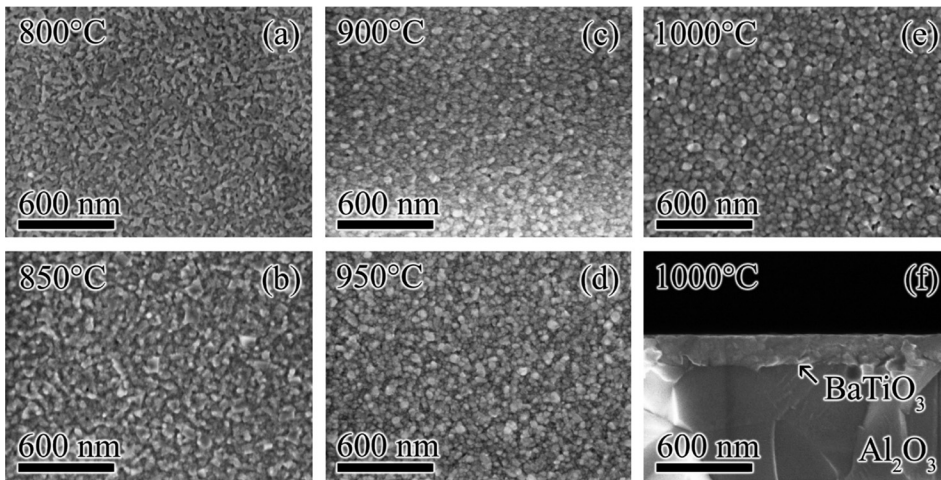


FIG. 2. Plan-view scanning electron micrographs of polycrystalline BaTiO<sub>3</sub> films annealed between (a) 800 °C and (e) 1000 °C. (f) is a cross-sectional image of the 1000 °C annealed BaTiO<sub>3</sub> film.

observed even for grain sizes as large as 63 nm. As expected, the epitaxial thin film sample shows a higher thermal conductivity than any nano-grained samples, but is a factor of two lower than the reported bulk values,<sup>8,18</sup> which is attributed mainly to film size effects. This coincides well with data taken by Foley *et al.*<sup>7</sup> on SrTiO<sub>3</sub> showing a similar dependence of thermal conductivity with grain size and a similar reduction from bulk values of approximately 11 W m<sup>-1</sup> K<sup>-1</sup> (Ref. 28).

The dependence of thermal conductivity on grain size shown in Fig. 3 illustrates limitation of the phonon mean free path spectrum by grain boundaries. With smaller grains, phonons with mean free paths greater than the grain sizes scatter more readily, translating into a reduced ability to conduct thermal energy. This is consistent with previous observations of nano-grained silicon<sup>29</sup> and our previous

measurements of grain size dependence on the thermal conductivity of SrTiO<sub>3</sub>.<sup>7</sup> The strong dependence of thermal conductivity on grain size greater than 40 nm implies phonons with mean free paths greater than 40 nm are conducting thermal energy. This directly conflicts with the picture that phonons in these complex oxides (e.g., BaTiO<sub>3</sub> and SrTiO<sub>3</sub>) have non-spectral (i.e., gray) mean free paths that are ~2 nm, which has been used to analyze phonon transport in SrTiO<sub>3</sub> previously.<sup>9</sup> The spectral nature of thermal conductivity in BaTiO<sub>3</sub> is illustrated by the model used in this study, shown in the inset of Fig. 3 (details of this model are described below). We see that with the nano-structured sample, the reduction in thermal conductivity arises from a limited contribution of the low frequency, long wavelength, phonons. At higher frequencies, the contribution to thermal conductivity is identical to bulk behavior.

Our model is based on semi-classical formalisms of the kinetic theory expression for thermal conductivity to model the spectral phonon transport and grain boundary scattering in our BaTiO<sub>3</sub> films. We approximate the phonon dispersion by a sine-type relation and only take contributions to the thermal conductivity from the acoustic branches of the phonon dispersion into account. Our model is based on the Kinetic Theory expression  $\kappa = C\nu\lambda/3 = C\nu^2\tau/3$ , where  $\kappa$  is the thermal conductivity,  $C$  is the heat capacity,  $\nu$  is the sound velocity,  $\lambda$  is the mean free path, and  $\tau$  is the scattering time. The boundary scattering is taken into account in the total scattering time by Matthiessen's rule given by

$$\frac{1}{\tau} = A\omega^2 \exp\left(\frac{-B}{T}\right) + D\omega^4 + \frac{\nu}{d_{film}} + \frac{\nu}{d_{gb}} \quad (1)$$

In this expression, from left to right, we account for the phonon-phonon scattering, impurity scattering, film thickness scattering, and grain boundary scattering, respectively. Here,  $T$  is the sample temperature,  $\omega$  is the phonon frequency,  $d$  is the appropriate thickness or grain size, and  $A$ ,  $B$ , and  $D$  are fitting parameters associated with the bulk scattering processes. These fitting parameters are determined initially by fitting the model to bulk, single crystal data<sup>18</sup> without the additional grain boundary and interface scattering components and are given as  $A = 700 \times 10^{-17} \text{ s K}^{-1}$ ,  $B = 165 \text{ K}$ , and  $D = 1 \times 10^{-35} \text{ s}^3$ .

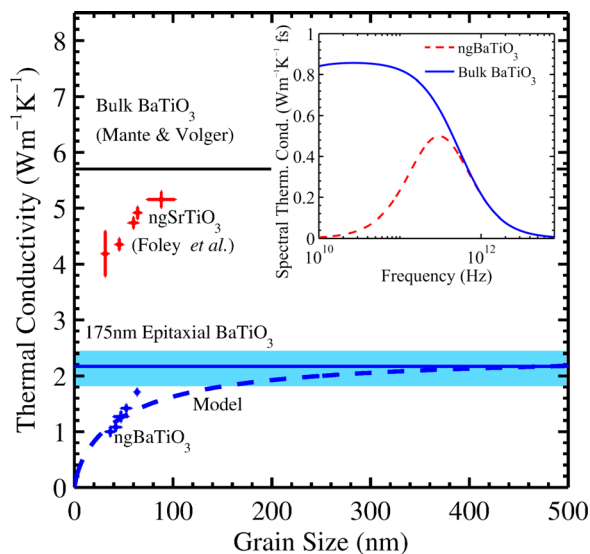


FIG. 3. Room temperature thermal conductivity of BaTiO<sub>3</sub> as a function of grain size along with the measured thermal conductivity of a single crystal film. For comparison, we also show the thermal conductivity of bulk, single crystal BaTiO<sub>3</sub> reported by Mante and Volger.<sup>18</sup> The dashed line represents our model calculations for BaTiO<sub>3</sub> as a function of grain size. Also included is similar data for another common perovskite, SrTiO<sub>3</sub>, from Foley *et al.*<sup>7</sup> The inset shows the spectral contribution to thermal conductivity with varying phonon frequency, highlighting the impact of nano-structuring to low frequency phonons.

As a comparison, and to accentuate the validity of our spectral model, we turn to a simple gray model for thermal conductivity which treats all phonons as having one mean free path at a given temperature. Using the same starting point of  $\kappa = Cv\lambda/3$ , and literature values for the heat capacity and thermal conductivity, we determine the gray mean free path of this system to be  $\sim 2$  nm, much less than the average grain size of any of the samples measured. The details of this calculation and resulting model can be found in the supporting material.<sup>19</sup>

We see in the included figures that our spectral model, which fits the measured data trend well, is more appropriate than the gray model (see supplementary material for a graphical comparison, including the gray model in Fig. S3) and asymptotes towards our single crystalline measured values at large grain sizes. Furthermore, this agreement with a sine-type dispersion model of the acoustic phonon modes indicates that the optical modes and more complex soft modes in the system do not significantly contribute to the thermal conductivity. In our model, we assume that both grain boundaries and film boundaries will scatter phonons equally, which accurately predicts that the epitaxial film data have a phonon mean free path limitation of the film thickness of the sample.

The thermal conductivity as a function of temperature of three samples is plotted in Fig. 4. Also for comparison in Fig. 4, we plot the bulk data from Mante and Volger.<sup>18</sup> The temperature trends among the epitaxial thin film and the two nano-grained samples (average grain sizes of 36 and 63 nm) are nearly equivalent, which is the expected trend in boundary scattering limited transport and is illustrated by the included model of the system. Expanded upon in the supplementary material,<sup>19</sup> the agreement of our spectral model of thermal conductivity and the measured data, especially when compared with a gray model, points clearly towards grain size effects directly limiting the phonon spectrum.

In bulk systems, low temperature thermal conductivity is limited by boundary and impurity scattering effects, and there is generally an increase in thermal conductivity until thermal energy increases the population of phonons in the system to

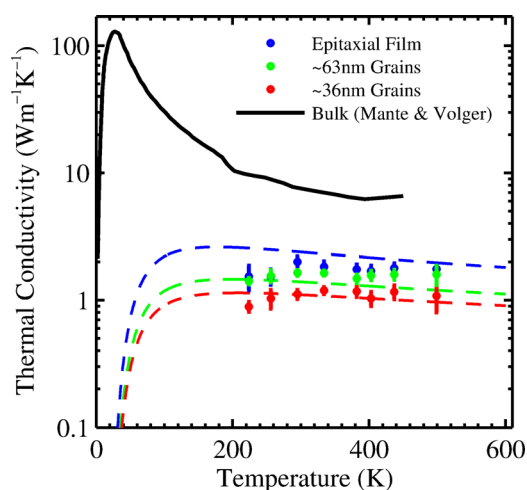


FIG. 4. Thermal conductivity of BaTiO<sub>3</sub> over varying sample temperature for two nano-grained and a single crystal thin film with respective modeled trends. For reference, bulk BaTiO<sub>3</sub> data from Mante and Volger has also been included.<sup>18</sup>

the point where phonon-phonon scattering becomes dominant. This causes the characteristic hump and subsequent decrease in thermal conductivity that is inversely proportional to temperature. Upon introduction of nanoscale scattering sites, such as grain boundaries, the boundary scattering effects are so severe that the characteristic hump gets smeared out into the modeled trend shown in Fig. 4. At somewhat higher temperatures, the boundaries have essentially stabilized the temperature dependence of the system and hold the thermal conductivity relatively constant over that range in temperature. This trend has been well studied in silicon-based nano structures<sup>30</sup> and extends as well into complex oxides.

Another important variation from bulk temperature dependence of BaTiO<sub>3</sub> seen in the nano-grained samples is the behavior around phase transition temperatures. The bulk phase transition progression of BaTiO<sub>3</sub> is well known,<sup>31</sup> with transitions from the rhombohedral, to orthorhombic, to tetragonal, and finally to the cubic phase at 180 K, 270 K, and 400 K, respectively. In bulk systems, thermal conductivity and heat capacity have been shown spike through these transition temperatures,<sup>18,32</sup> but in our nano-structured system, we do not observe any measurable nonlinearities or inflections across these temperatures. It is well demonstrated in both bulk ceramics<sup>33–35</sup> and thin films<sup>20</sup> that as grain size is decreased below 1  $\mu$ m, the phase transitions tend to pinch together and diminish in their amplitude. Using a metric of the dielectric constant, Frey *et al.*<sup>36</sup> were able to show a clear low temperature phase transition in BaTiO<sub>3</sub> samples that had grain sizes on the order of 1  $\mu$ m, yet the peak in dielectric constant for grain sizes below 100 nm is suppressed nearly completely. Accompanying this suppression of peak permittivity was a decrease in the latent heat of transition at the Curie temperature.<sup>33</sup> Ihlefeld *et al.*<sup>20</sup> show this same relative permittivity trend as observed in bulk ceramics for thin film samples similar to those used in this study, with nearly full peak suppression at grain sizes of about 76 nm. While we know from previous work in similar systems<sup>20</sup> that these samples are still in a non-centrosymmetric crystal structured regime, since we observe no obvious influence of the orthorhombic to tetragonal or tetragonal to cubic phase transitions in both the single crystalline and nanograined films, we hypothesize that the fine grain and thin film geometries are suppressing the influence of these phase transitions on thermal conductivity.

In summary, the nano-grained samples of barium titanate showed a significantly reduced thermal conductivity compared with bulk. The thermal conductivity trended lower with decreasing grain sizes showing a limitation of phonon mean free paths by grain boundaries. Over a range of industry and material relevant temperatures, it is clear that the thermal conductivity of the samples no longer depends strongly on temperature, since the scattering component from grain boundaries dominates over any other contribution to overall phonon scattering and thermal conductivity.

The authors would like to acknowledge Bonnie McKenzie at Sandia National Labs for her help materials characterization and electron microscopy, as well as Christopher T. Shelton for help with the atomic force micrographs seen in the Supporting Material. We appreciate funding from the National Science Foundation (CBET-1339436), the Army Research Office,

Grant No. W911NF-13-1-0378, and the Air Force Office of Scientific Research under AFOSR Award No. FA9550-14-1-0067 (Subaward No. 5010-UV-AFOSR-0067). This work was also supported, in part, by the Laboratory Directed Research and Development (LDRD) program at Sandia National Laboratories. Sandia National Laboratories is a multi-program laboratory managed and operated by Sandia Corporation, a wholly owned subsidiary of Lockheed Martin Corporation, for the U.S. Department of Energy's National Nuclear Security Administration under Contract No. DE-AC04-94AL85000.

- <sup>1</sup>A. von Hippel, R. G. Breckenridge, F. G. Chesley, and L. Tisza, *Ind. Eng. Chem.* **38**, 1097 (1946).
- <sup>2</sup>S. Roberts, *Phys. Rev.* **71**, 890 (1947).
- <sup>3</sup>N. Nuraje and K. Su, *Nanoscale* **5**, 8752 (2013).
- <sup>4</sup>G. Jonker, *Solid-State Electron.* **7**, 895 (1964).
- <sup>5</sup>H. Kishi, Y. Mizuno, and H. Chazono, *Jpn. J. Appl. Phys. Part 1* **42**, 1 (2003).
- <sup>6</sup>M.-J. Pan and C. A. Randall, *IEEE Electr. Insul. Mag.* **26**, 44 (2010).
- <sup>7</sup>B. M. Foley, H. J. Brown-Shaklee, J. C. Duda, R. Cheaito, B. J. Gibbons, D. Medlin, J. F. Ihlefeld, and P. E. Hopkins, *Appl. Phys. Lett.* **101**, 231908 (2012).
- <sup>8</sup>M. Tachibana, T. Kolodiazny, and E. Takayama-Muromachi, *Appl. Phys. Lett.* **93**, 092902 (2008).
- <sup>9</sup>Y. Wang, K. Fujinami, R. Zhang, C. Wan, N. Wang, Y. Ba, and K. Koumoto, *Appl. Phys. Express* **3**, 031101 (2010).
- <sup>10</sup>S. Bhattacharya, A. Mehdizadeh Dehkordi, S. Tennakoon, R. Adebisi, J. R. Gladden, T. Darroudi, H. N. Alshareef, and T. M. Tritt, *J. Appl. Phys.* **115**, 223712 (2014).
- <sup>11</sup>S. M. Aygun, J. F. Ihlefeld, W. J. Borland, and J.-P. Maria, *J. Appl. Phys.* **109**, 034108 (2011).
- <sup>12</sup>P. E. Hopkins, J. R. Serrano, L. M. Phinney, S. P. Kearney, T. W. Grasser, and C. T. Harris, *J. Heat Transfer* **132**, 081302 (2010).
- <sup>13</sup>D. G. Cahill, *Rev. Sci. Instrum.* **75**, 5119 (2004).
- <sup>14</sup>A. J. Schmidt, X. Chen, and G. Chen, *Rev. Sci. Instrum.* **79**, 114902 (2008).
- <sup>15</sup>A. Jezowski, J. Mucha, R. Pazik, and W. Strek, *Appl. Phys. Lett.* **90**, 114104 (2007).
- <sup>16</sup>S. T. Davitadze, S. N. Kravchun, B. A. Strukov, B. M. Goltzman, V. V. Lemanov, and S. G. Shulman, *Appl. Phys. Lett.* **80**, 1631 (2002).
- <sup>17</sup>G. Chen, *Phys. Rev. B* **57**, 14958 (1998).
- <sup>18</sup>A. Mante and J. Volger, *Phys. Lett. A* **24**, 139 (1967).
- <sup>19</sup>See supplementary material at <http://dx.doi.org/10.1063/1.4893920> for more information regarding background and analysis.
- <sup>20</sup>J. F. Ihlefeld, A. M. Vodnick, S. P. Baker, W. J. Borland, and J.-P. Maria, *J. Appl. Phys.* **103**, 074112 (2008).
- <sup>21</sup>C. T. Shelton, P. G. Kotula, G. L. Brennecke, P. G. Lam, K. E. Meyer, J.-P. Maria, B. J. Gibbons, and J. F. Ihlefeld, *Adv. Funct. Mater.* **22**, 2295 (2012).
- <sup>22</sup>S. M. Aygün, P. Daniels, W. J. Borland, and J.-P. Maria, *J. Mater. Res.* **25**, 427 (2010).
- <sup>23</sup>G. Koster, B. L. Kropman, G. J. H. M. Rijnders, D. H. A. Blank, and H. Rogalla, *Appl. Phys. Lett.* **73**, 2920 (1998).
- <sup>24</sup>A. R. Kortan, M. Hong, J. Kwo, J. P. Mannaerts, and N. Kopylov, *Phys. Rev. B* **60**, 10913 (1999).
- <sup>25</sup>H. Megaw, *Nature* **155**, 484 (1945).
- <sup>26</sup>R. E. Newnham and Y. M. de Haan, *Z. Kristallogr.* **117**, 235 (1962).
- <sup>27</sup>ASTM Standard E112, "Standard Test Method for Determining Average Grain Size," *ASTM International*, Vol. 03.01, (2013).
- <sup>28</sup>Y. Suemune, *J. Phys. Soc. Jpn.* **20**, 174 (1965).
- <sup>29</sup>Z. Wang, J. E. Alaniz, W. Jang, J. E. Garay, and C. Dames, *Nano Lett.* **11**, 2206 (2011).
- <sup>30</sup>A. M. Marconnet, M. Asheghi, and K. E. Goodson, *J. Heat Transfer* **135**, 061601 (2013).
- <sup>31</sup>A. von Hippel, *Rev. Mod. Phys.* **22**, 221 (1950).
- <sup>32</sup>G. Shirane and A. Takeda, *J. Phys. Soc. Jpn.* **7**, 1 (1952).
- <sup>33</sup>M. H. Frey and D. A. Payne, *Phys. Rev. B* **54**, 3158 (1996).
- <sup>34</sup>G. Arlt, D. Hennings, and G. de With, *J. Appl. Phys.* **58**, 1619 (1985).
- <sup>35</sup>K. Kinoshita and A. Yamaji, *J. Appl. Phys.* **47**, 371 (1976).
- <sup>36</sup>M. H. Frey, Z. Xu, P. Han, and D. A. Payne, *Ferroelectrics* **206**, 337 (1998).